10th ECCOMAS Thematic Conference on Computational Methods in Structural Dynamics and Earthquake Engineering M. Papadrakakis, M. Fragiadakis (eds.) Rhodes Island, Greece, 15-18 June 2025

FINITE ELEMENT ANALYSIS OF SELF-CENTRING BEAM-TO-COLUMN SUBASSEMBLIES IN SEISMIC-RESILIENT STEEL MRF: PRELIMINARY EVALUATION OF THE FRAME EXPANSION EFFECTS

A. Roumieh¹, L. Kauntz Moderini¹, E. Elettore¹, S. Di Benedetto², A.B. Francavilla³, M. Latour², F. Gutiérrez-Urzúa^{1,4}, L. Pieroni¹, S. Ramhormozian⁵, B. Simpson⁶, A.R. Barbosa⁷, G. Rizzano², D. Grant⁸, F. Ribeiro⁹, A.A. Correia⁹, F. Freddi¹

¹ University College London address

e-mail: {ali.roumieh.23, leo.moderini.18, e.elettore, ludovica.pieroni.20, f.freddi}@ucl.ac.uk

² University of Salerno address {sdibenedetto, mlatour, g.rizzano}@unisa.it

³ Pegaso University address {antonellabianca.francavilla}@unipegaso.it

⁴ AtkinsRéalis address {fernando.gutierrezurzua}@atkinsrealis.com

⁵ Auckland University of Technology address {shahab.ramhormozian}@aut.ac.nz

> ⁶ Stanford University address {bsimpson}@stanford.edu

Oregon State University address Andre.Barbosa @ oregonstate.edu

⁸ Arup address {Damian.Grant}@arup.com

⁹ National Laboratory for Civil Engineering (LNEC) address {flribeiro, aacorreia}@lnec.pt

Abstract

Conventional code-based seismic design methods widely applied worldwide rely on the dissipation of seismic energy through construction damage. While this approach ensures life safety, it often results in significant post-earthquake damage, leading to substantial direct and indirect losses that affect communities' resilience. To overcome these limitations, modern Earthquake Engineering is focusing on developing high-performance, cost-effective structures capable of withstanding design-level earthquakes with minimal socio-economic impact. In this context, the ERIES – SC-RESTEEL (Self-Centring seismic-RESilient sTEEL structures) project explores the structural response, repairability, resilience, and performance recovery of a steel self-centring Moment-Resisting Frame (MRF) incorporating friction devices and post-tensioned bars at column bases and beam-to-column joints. The project includes full-scale shaking table tests on a three-storey steel MRF at LNEC (Laboratório Nacional de Engenharia Civil) in Lisbon, Portugal. Moreover, the project investigates the response of the beam-to-column joint and the effect of the frame expansion due to the rocking of the beams through quasi-static cyclic tests on MRF subassemblies in Salerno, Italy. This paper illustrates the preparatory numerical work, including advanced Finite Element (FE) models in ABAQUS considering two configurations of the subassemblies, and investigates a solution to mitigate the frame expansion effects. The combined FE and experimental results provide crucial insights into the design of shaking table tests and the expected experimental outcomes.

Keywords: Self-centring Moment-Resisting Frames, Beam-to-Column Joints, Finite Element Modelling, Frame Expansion.

1 INTRODUCTION

Earthquakes rank among the most devastating and costly natural disasters worldwide. Conventional seismic design methodologies, as recommended by most current building codes (*e.g.*, Eurocode 8 [1]), primarily rely on structural damage to dissipate seismic energy and meet the life safety requirements. However, such an approach often leaves buildings heavily damaged after earthquakes, leading to significant direct (*e.g.*, casualties, repair expenses) and indirect losses (*e.g.*, operational downtime). These consequences are particularly significant after 'rare' seismic events, which adversely affect the resilience of communities, especially when the damaged structures are critical facilities that must remain functional after a disaster. To address these limitations, modern Earthquake Engineering is advancing in the development of seismic-resilient structures able to minimise both seismic damage and repair time, thereby reducing socio-economic impacts following severe earthquakes [2]. To this end, one effective strategy is based on the use of seismic devices, which have been extensively studied and are now widely used in construction. Well-established solutions are based on supplemental damping [3]-[5] and seismic isolation systems [6] [7]. Additional innovative strategies, such as rocking and spine low-damage systems [8]-[10], have recently gained recognition for their distinct advantages.

In the case of steel Moment Resisting Frames (MRFs), a promising solution involves incorporating Friction Devices (FDs) into Beam-to-Column Joints (BCJs) and/or Column Bases (CBs). This approach enables high local ductility and energy dissipation while ensuring minimal damage, as the affected components are designed to be easily repairable or replaceable [11]-[13]. However, reducing structural damage alone does not necessarily guarantee repairability. Post-earthquake residual drifts can exceed acceptable limits, often recommended to be within the range of 0.5% or 1% for repairable buildings and 0.2% for buildings requiring

structural realignment [14]. This challenge has been addressed by integrating elastic restoring forces to enhance the Self-Centring (SC) capability of structures. SC systems, which effectively reduce residual deformations, have been extensively investigated across various structural typologies and materials, such as bridge piers [15], reinforced concrete structures [16], steel braced frames [17][18] and steel MRFs [19]-[22].

For steel MRFs, one strategy involves incorporating self-centring devices into BCJs [8][23] [24] and/or CBs [21][22][25]. Self-centring BCJs typically include Post-Tensioned (PT) steel bars, which are aligned parallel to the beams and anchored externally to control the gap-opening mechanisms (*i.e.*, rocking) at the connection interface. Seismic energy is typically dissipated through replaceable yielding devices or FDs [26] integrated into the connection.

Within this context, the ERIES – SC-RESTEEL (Self-Centring Seismic-RESilient STEEL Structures) project aims to advance knowledge and drive innovation through experimental investigations into the seismic performance, repairability, and effective integration of self-centring devices in steel MRFs. This approach incorporates dissipative and self-centring components at CBs and BCJs to dissipate seismic energy and eliminate residual drifts.

As previously mentioned, incorporating self-centring devices into BCJs promotes repairability. However, the rocking mechanism of the beams may induce frame expansion effects, hindering the joint's self-centring capability, increasing the demands on the floor slab and columns [27], and causing irreparable damage. To address this issue, several research works have focused on developing solutions to mitigate the effects of the frame expansion. Among others, Deng *et al.* [28] investigated a configuration where the central rocking part of the beam is fully restrained for the bending actions but is provided with a horizontal gap to accommodate beam elongation. Similarly, Garlock *et al.* [29] suggested using collector beams designed to deform and transfer loads to the frames, thereby reducing the impact of the frame expansion. However, it was observed that the presence of collector beams, which are prone to yielding, could lead to secondary damage, including a significant contribution to the axial force in the beams, and compromise structural integrity.

This paper addresses the aforementioned issues by proposing and investigating a solution to prevent beam elongation in steel MRFs equipped with SC-BCJs. This solution consists of SC-BCJs equipped with short PT bars and disc springs, along with a splice mechanism at the beam's midspan, to mitigate the frame expansion effect. The study examines the performance of a single-bay frame subassembly extracted from the second storey of a three-storey structure and utilises advanced Finite Element (FE) analyses in ABAQUS to investigate the response of the conventional and the proposed solution. FE models have been developed considering two frame configurations, with and without the central splice. The preliminary numerical simulations presented in this paper enable the evaluation of the proposed solution's performance. On the other hand, they provide the necessary information for designing the experimental campaign that will be conducted at the STRENGTH laboratory (Structural Engineering Test Hall) at the University of Salerno as part of the ERIES – SC-RESTEEL project.

This paper outlines the design and concept of the SC-BCJ and the splice mechanism at the beam's midspan under study, illustrates the case study frame, the FE modelling approach, and the preliminary results obtained. The numerical results are presented for both monotonic and cyclic loading scenarios of the two frame configurations, highlighting the benefits of the proposed solution.

2 SELF-CENTRING BEAM-TO-COLUMN JOINTS (SC-BCJS)

2.1 Concept

Figure 1(a) shows the SC-BCJ investigated in this study. It includes angle cleat connections with L-plates bolted to the column flanges and the beam, together with friction shims placed between the L-plates and the beam flange and pre-stressed by high-strength bolts. As shown in Figure 1(b), the L-plates and FDs are made with round holes, while the beam flanges include slotted holes to allow the relative slippage of the plates forming the friction surface. Moreover, the joint includes a system of two PT bars with disc springs clamped from one side to the column flange and from the other side to an anchorage plate welded at a specific distance between the beam's flanges. The system of disc springs can be arranged in series and in parallel to optimally calibrate the strength and stiffness of the self-centring system. The FDs and PT bars provide, respectively, the energy dissipation and self-centring capacity of the connection.

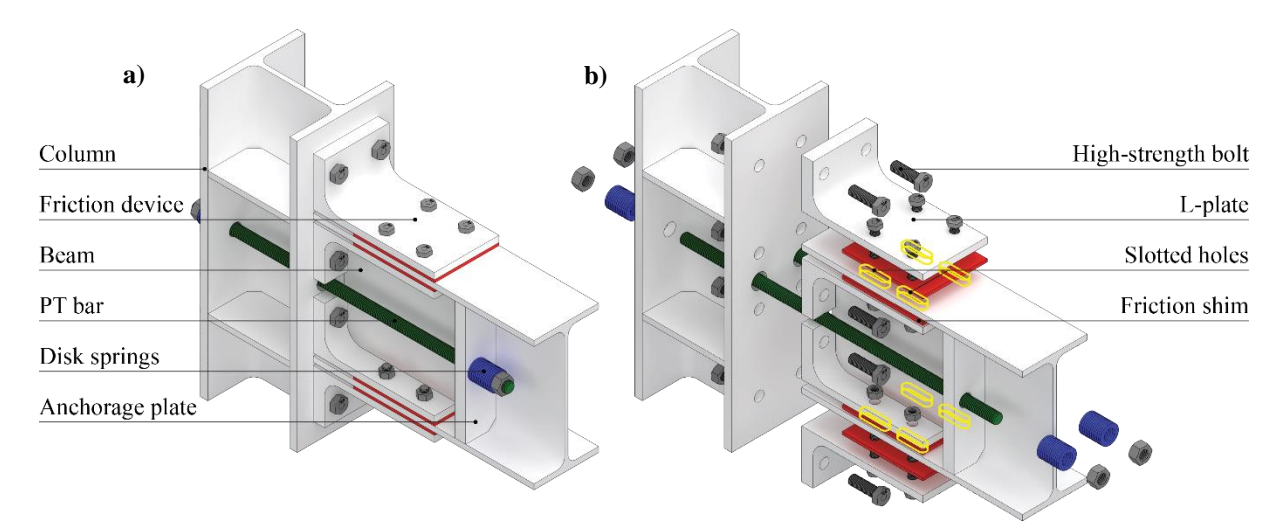


Figure 1: Self-Centring Beam-to-Column Joint: a) 3D view; b) 3D exploded view.

2.2 Force distribution in the connection

During high-intensity earthquakes, the SC-BCJ is subjected to bending moments inducing the rocking mechanism and generating a distribution of forces in the FDs, and PT bars. The force developed in the FDs (F_{FD}) can be calculated as follows:

$$F_{FD} = \mu \, n_S \, n_b \, F_p \tag{1}$$

where μ is the friction coefficient; n_S is the number of friction surfaces (*i.e.*, two surfaces at each flange in the proposed configuration); n_b is the number of bolts connected at each surface; F_p is the preload force applied to each bolt. The parameters μ and F_p , and hence also the slippage force, are expected to remain approximately constant during the rocking motion.

The force in the PT bar (F_{PT}) is defined by an initial post-tensioning force $(F_{PT,0})$, which increases during the rocking motion as a consequence of the PT bars elongation (ΔF_{PT}) . The forces in the PT bars can be calculated as follows:

$$F_{PT,0} = n_{PT}F_{n,PT}$$
; $\Delta F_{PT} = K_{eq}\Delta_{el,PT}$; $F_{PT} = F_{PT,0} + \Delta F_{PT}$ (2)

where n_{PT} is the total number of PT bars, $F_{p,PT}$ is the initial preload force in each bar; K_{eq} is the stiffness for the whole system composed of PT bars and disc springs; and $\Delta_{el,PT}$ is the PT bars elongation. The stiffness of the PT bar system is calculated as follows:

$$K_{eq} = n_{PT} \frac{K_{PT} K_{DS}}{K_{PT} + K_{DS}} \; ; \; K_{PT} = \frac{E_{PT} A_{res}}{L_{PT}} ; \; K_{DS} = \frac{n_{par}}{n_{ser}} K_{DS,single}$$
 (3)

where K_{PT} is the stiffness of a single PT bar; K_{DS} is the stiffness of the whole set of disc springs in parallel and in series; n_{PT} is the total number of PT bars in the system; E_{PT} is the elastic modulus of the PT bar; A_{res} is the resistance area of the PT bar; L_{PT} is the length of the PT bars; n_{par} is the number of disc springs in parallel; and n_{ser} is the number of disc springs in series.

The maximum force in the PT bars can be easily calculated based on the target rotation for the joint (θ_{target}). This can be assumed based on code recommendations (e.g., 40 mrad according to the Eurocode 8 [1], and allows calculating $\Delta_{el,PT}$ as follows:

$$\Delta_{el,PT} = \theta_{target} \frac{h_{eff}}{2} \tag{4}$$

where $h_{eff} = h_b - t_f$ where h_b and t_f are the beam's height and flange thickness, respectively.

2.3 Moment-rotation relationship

Figure 2(a) shows a deformed configuration and the rocking mechanism of an SC-BCJ. The forces in each component are calculated by imposing a static equilibrium at the centre of rotation (COR). F_C represents the compression force, F_F represents the sliding forces in the friction pads at the beam flanges, while F_{PT} is the sum of the forces provided by the system of PT bars and disc springs. Figure 2(b) shows the analytical moment-rotation behaviour of the joint. This is a function of the response of each of the joint's components during rocking.

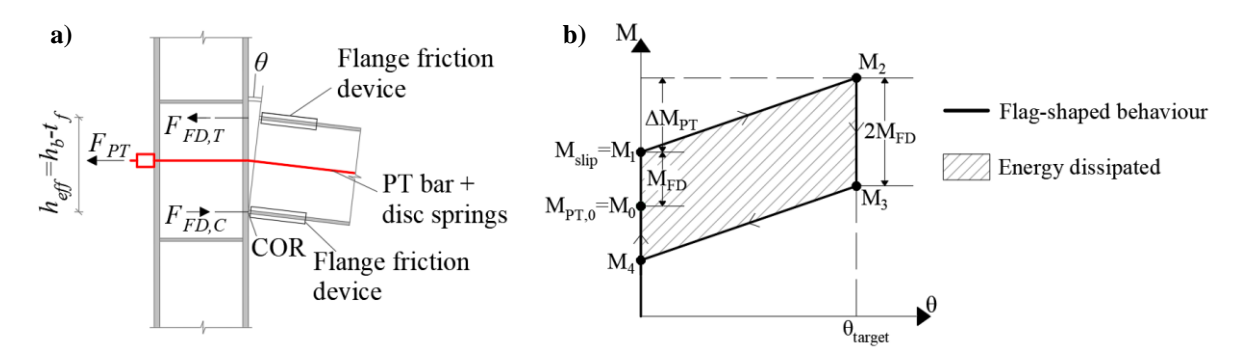


Figure 2 a) Force distribution in the joint during rocking; b) Analytical moment-rotation behaviour of the SC-BCJ.

The moment M_0 results from the initial post-tensioning force of the PT bar as follows:

$$M_{PT,0} = M_0 = F_{PT,0} \frac{h_{eff}}{2} \tag{5}$$

The moment M_{FD} is provided by the FDs and is calculated as follows:

$$M_{FD} = F_{FD} h_{eff} (6)$$

The slippage moment $M_{slip} = M_1$ corresponds to the activation of the friction pads and is calculated as follows:

$$M_{slip} = M_1 = M_0 + M_{FD} (7)$$

 M_2 is the maximum moment provided at the target rotation (θ_{target}), and results from the slippage moment and the additional moment resulting from the PT bars hardening ΔM_{PT} :

$$\Delta M_{PT} = \Delta F_{PT} \frac{h_{eff}}{2} \tag{8}$$

$$M_2 = M_0 + M_{FD} + \Delta M_{PT} \tag{9}$$

The unloading moments M_3 and M_4 are calculated at the target and zero rotation respectively as follows:

$$M_3 = M_2 - 2M_{FD} (10)$$

$$M_4 = M_1 - 2M_{FD} (11)$$

3 CASE STUDY AND FINITE ELEMENT MODELLING

3.1 Case study structure

Shake table tests will be conducted on a large-scale, three-storey steel moment-resisting frame. The prototype structure features three bays along both the x- and y-directions and is scaled using material and acceleration identity with a scaling factor $\lambda = 0.6$. The specimen for the subassembly is extracted from this scaled prototype, as shown in Figure 3.

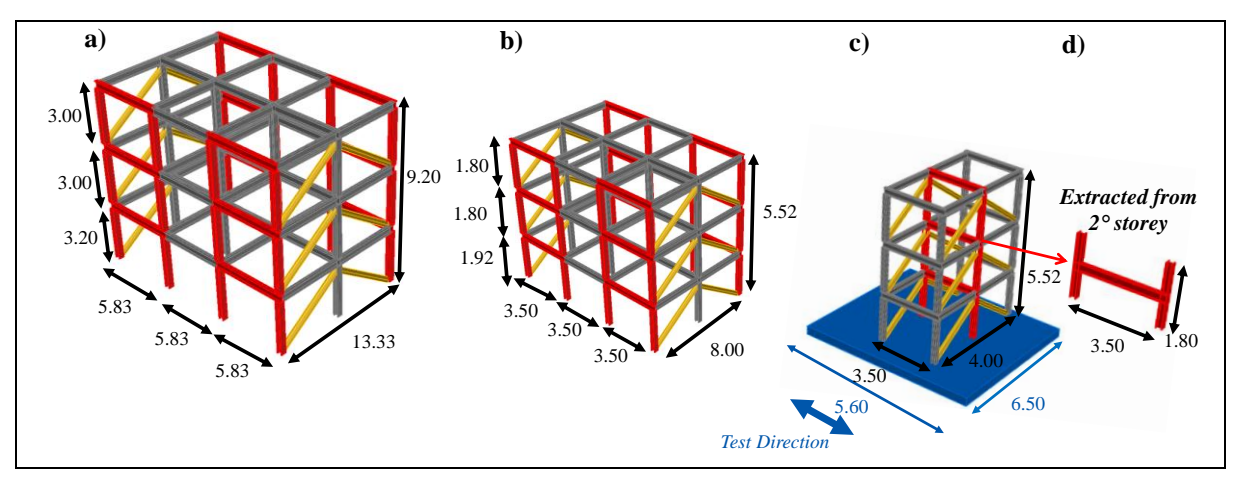


Figure 3: 3D view of: a) Prototype structure; b) Scaled structure; c) Specimen for the shaking table tests; d) Subassembly for the quasi-static tests [Dimensions in m].

3.2 Single-bay frame subassembly

The subassembly consists of a single-bay frame representing the second storey of the test specimen, as shown in Figure 4. Experimental tests will be conducted on two frame configurations. The first configuration (Figure 4(a)) includes SC-BCJs and a continuous beam. The second configuration (Figure 4(b)) includes the same SC-BCJs and a splice mechanism at the beam's midspan. The splice consists of bolted plates connected to the beams' webs and flanges. Slotted holes are included in the beam, and a teflon material, characterised by a low friction coefficient, is included between the plates to create a 'frictionless' interface. This mechanism enables the reduction of axial forces in the beams, thereby mitigating the frame expansion effect, allowing for a more controlled response of the SC-BCJs, and reducing damage to the joint components. Columns are pinned at the base and the upper side, simulating the zero moment at the columns' mid-height, as expected in the three-storey frame. At the upper side, columns are connected by a tube, acting as a pendulum, so that lateral loading is applied to one column using a hydraulic actuator and transferred to the other through the pendulum system. Additionally, a

separate test setup (not shown in the figure) is used to restrain the columns' out-of-plane displacement.

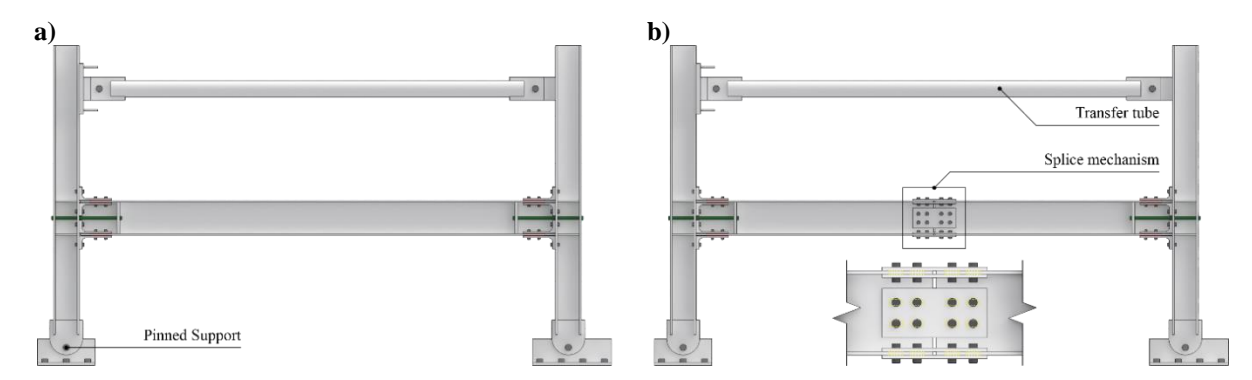


Figure 4: Tested Subassemblies with: a) Continuous beam; b) Splice at midspan.

3.3 Experimental program

Quasi-static tests will be conducted on both configurations. The specimens will undergo progressively increasing cyclic loading until reaching a target joint rotation of 0.04 rad in accordance with AISC 341-16 [33] section K2.4b provisions. This approach ensures a thorough evaluation of the joint's rotational capacity, replicating the repeated cyclic effects experienced in a real-life seismic event.

3.4 Finite Element (FE) modelling

Advanced 3D FE models of the subassemblies have been developed in ABAQUS. All the components are modelled using the eight-node linear brick element (*i.e.*, C3D8R) available in ABAQUS. Elements C3D8R rely on 'reduced integration' and 'hourglass control'. The steel material model follows a multilinear stress-strain law for all components, except for the bolts and PT bars, where a bilinear stress-strain law was used. Interaction properties were modelled using 'surface-to-surface' contact, employing 'hard contact' and 'penalty' contacts to simulate normal and tangential response, respectively. The 'bolt load' option was used to model the preload force for both bolts and PT bars. The preload was assigned through the 'apply force' option at the initial stage, and then it was allowed to vary during the analyses by using the 'fixed at current length' option. Columns were pinned at the base by restraining them in all three inplane directions (i.e., U1=0, U2=0, U3=0, UR2=0, UR3=0). The analyses were performed in two steps i) bolts and PT bars preload, and ii) application of the displacement history.

Figure 5 shows the three models developed in ABAQUS. Figure 5(a) shows the model of the single BCJ. Figure 5(b) and (c) show the two configurations of the single-bay frame with and without the splice mechanism at the beam's midspan. All models were initially analysed under monotonic displacements and successively, under a cyclic analysis with a single cycle up to the joint target rotation. The comparison of the moment-rotation response of the three models provides some insights into the effectiveness of the splice mechanism in mitigating the frame expansion effects.

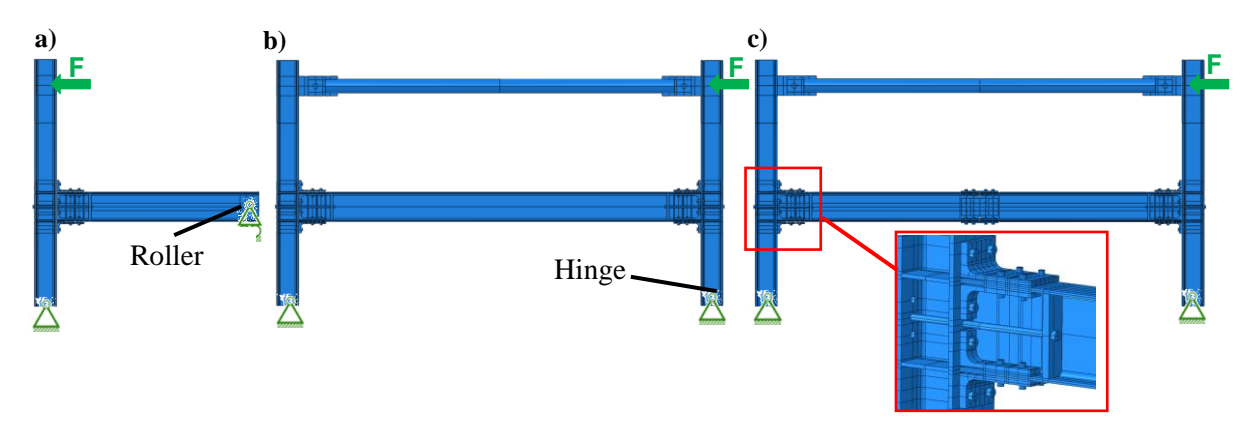


Figure 5: ABAQUS models: a) Single BCJ; b) Single-bay with continuous beam; c) Single-bay with splice.

4 RESULTS

Figure 6 shows a comparison of the monotonic analysis for the three models. Figure 6(a) shows that the three models exhibit similar slippage moments, corresponding to the activation of the FDs. The configuration featuring the splice shows a moment-rotation response almost identical to the single BCJ, demonstrating a limited to no influence of the frame expansion effects. Conversely, the frame with the continuous beam exhibits a significantly larger moment compared to the single BCJ. Additionally, the results highlight that the BCJ with the continuous beam experiences higher stresses due to the high axial force developed in the beam during the corresponding higher moment. For the target joint rotation of 0.04 rad, such stresses exceed the yielding stress of steel. Figure 6(b) illustrates the axial force variability with increasing rotations, highlighting the beneficial effects provided by the splice. The frame with the splice exhibits a constant, negligible axial force. Conversely, the frame with the continuous beam exhibits a sharp increase in the axial force, reaching high values. This axial force leads to plastic damage, hinders structural integrity and compromises the BCJ's self-centring capability.

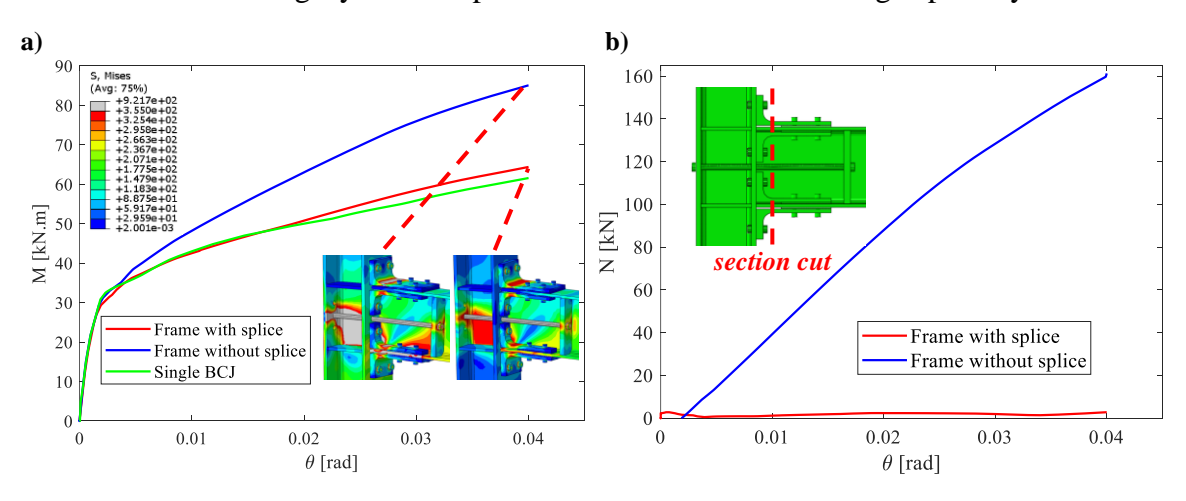


Figure 6: Comparisons of BCJ behaviour in terms of: a) Moment-rotation curves and von Mises stresses from the ABAQUS models [units of colour bar in MPa]; b) Axial force evolution between the two frame configurations.

Figure 7 shows the moment-rotation cyclic response of the two frame configurations. The results show a slightly better self-centring capability for the frame with the splice. The benefits are limited in this configuration but are expected to be more pronounced in other configurations with different forces in the PT bars and FDs, as well as in multiple bays where the displacements related to the frame expansion accumulate at each frame. Figure 7(b) and (c) shows the stresses

distribution for the BCJs for the frames without and with splice, respectively, at maximum displacement. It is noted that for the frame without the splice, the BCJ reaches higher stresses exceeding the yielding stress of the steel material, especially at the column web and beam flange. These findings highlight the critical role of the splice mechanism in preventing excessive yielding in critical structural components, thereby reducing plastic deformation, ensuring self-centring capability, a more controlled structural response, and mitigating frame expansion.

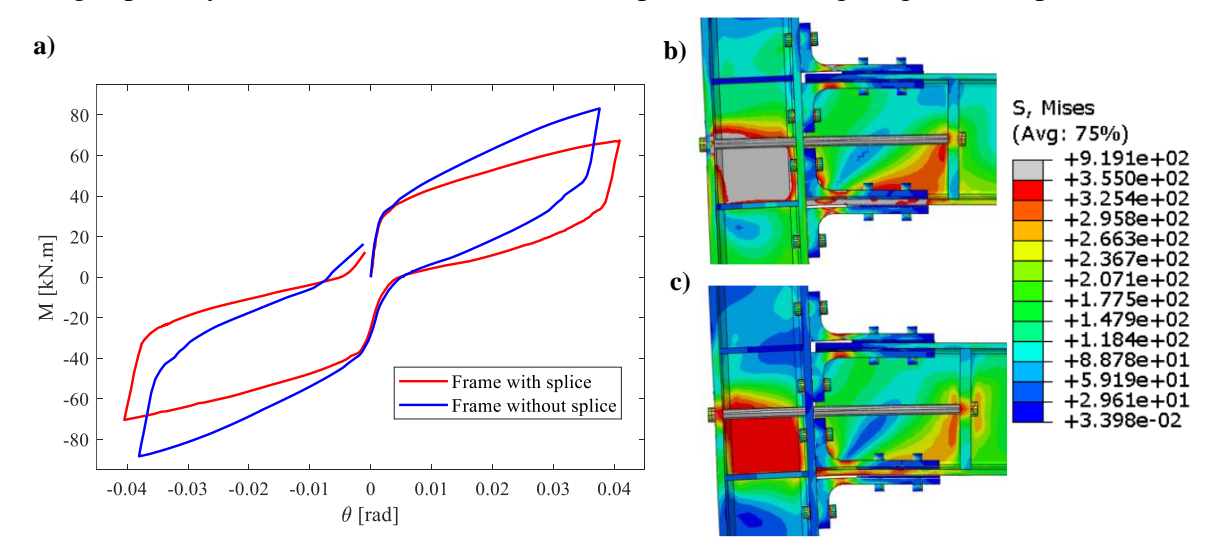


Figure 7: a) Cyclic moment-rotation curve comparison between the two frame configurations; and von Mises stresses contours for b) frame without splice; c) frame with splice. [units of colour bar in MPa].

5 CONCLUSIONS

As part of the ERIES SC-RESTEEL project, shake table tests will be conducted on a large-scale, three-storey steel moment-resisting frame featuring self-centring beam-to-column joints and column bases. This paper presents the design and finite element modelling of beam-to-column subassemblies that will be tested at the STRENGTH (Structural Engineering Test Hall) laboratory of the University of Salerno and that will be used in the specimen of the shaking table tests. The primary focus is on investigating a solution to address the frame expansion effect resulting from the rocking of the beams. Such effects lead to high axial forces and 'unexpected' moments that can compromise structural integrity. The proposed solution includes a splice mechanism at midspan allowing slippage and, hence, the shortening of the beam. Finite element models have been developed in ABAQUS to compare two frame configurations. The findings offer valuable insights into the performance of the proposed self-centring beam-to-column joints and highlight the effectiveness of the proposed solution in mitigating the frame expansion effects, thus, reducing damage to the joint and enhancing the self-centring behaviour. The numerical results provided significant support for designing the experimental tests.

6 ACKNOWLEDGEMENT

This work is part of the transnational access project "ERIES – SC-RESTEEL", supported by the Engineering Research Infrastructures for European Synergies (ERIES) project (www.eries.eu), which has received funding from the European Union's Horizon Europe Framework Programme under Grant Agreement No. 101058684. This is ERIES publication number C23.

REFERENCES

- [1] EN 1998-1, Eurocode 8: Design of structures for earthquake resistance Part 1: General rules, seismic actions and rules for buildings, European Committee for Standardization, Brussels.
- [2] Freddi, F., Galasso, C., Cremen, G., Dall'Asta, A., Di Sarno, L., Giaralis, A., Gutiérrez-Urzúa, L.F., Málaga-Chuquitaype, C., Mitoulis, S., Petrone, C., Sextos, A., Sousa, L., Tarbali, K., Tubaldi, E., Wardman, J., Woo, G. Innovations in Earthquake Risk Reduction for Resilience: Recent Advances and Challenges. *International Journal of Disaster Risk Reduction*, **60**, 102267, 2021.
- [3] Symans M.D., Charney F.A., Whittaker A.S., Constantinou M.C., Kircher C.A., Johnson M.W., McNamara R.J. Energy dissipation systems for seismic applications: Current practice and recent developments. *Journal of Structural Engineering*, **134**(1), 3–21, 2008.
- [4] Seo C.Y., Karavasilis T.L., Ricles J.M., Sause R. Seismic performance and probabilistic collapse resistance assessment of steel moment resisting frames with fluid viscous dampers. *Earthquake Engineering & Structural Dynamics*, **43**(14), 2135-2154, 2014.
- [5] Gutiérrez-Urzúa L.F., Freddi F. Influence of the design objectives on the seismic performance of steel moment resisting frames retrofitted with buckling restrained braces. *Earth-quake Engineering & Structural Dynamics*, **51**(13), 3131–3153, 2022.
- [6] Grant D., Fenves G., Whittaker A. Bidirectional modelling of high-damping rubber bearings. *Journal of Earthquake Engineering*, **8**(1), 161-185, 2004.
- [7] Calvi P.M., Calvi G.M. Historical development of friction-based seismic isolation systems. *Soil Dynamics and Earthquake Engineering*, **106**, 14-30, 2018.
- [8] Ricles J., Sause R., Garlock M., Zhao C. Post-tensioned Seismic-Resistant Connections for Steel Frames. *Journal of Structural Engineering*, **127**(2), 113–121, 2001.
- [9] Blomgren, Hans-Erik; Pei, Shiling, Jin, Zhibin; Powers, Josh; Dolan, James D.; Van De Lindt, John W.; Barbosa, Andre R.; Huang D. Full-Scale Shake Table Testing of Cross-Laminated Timber Rocking Shear Walls with Replaceable Components. *Journal of Structural Engineering*, **145**(101), 04019115, 2019.
- [10] Simpson B.G., Rivera Torres D. Simplified Modal Pushover Analysis to Estimate First-And Higher-Mode Force Demands for Design of Strongback-Braced Frames. *Journal of Structural Engineering*, **147**(12), 04021196, 2023.
- [11] Grigorian C.E., Yang T.S., Popov E.P. Slotted bolted connection energy dissipators. *Earthquake Spectra*, **9**(3), 491-504, 1993.
- [12] Latour M., D'Aniello M., Zimbru M., Rizzano G., Piluso V., Landolfo R. Removable friction dampers for low-damage steel beam-to-column joints. *Soil Dynamics and Earth-quake Engineering*, **115**, 66-81, 2018.
- [13] Di Benedetto S., Francavilla A.B., Latour M., Piluso V., Rizzano G. Experimental response of a large-scale two-storey steel building equipped with low-yielding friction joints. *Soil Dynamics and Earthquake Engineering*, **152**, 107022, 2022.

- [14] FEMA P58-1. (2012). Seismic performance assessment of buildings. Volume 1 Methodology. Applied Technology Council, Redwood City, CA.
- [15] Shen Y., Freddi F., Li Y., Li J. Enhanced Strategies for Seismic Resilient Posttensioned Reinforced Concrete Bridge Piers: Experimental Tests and Numerical Simulations. *Journal of Structural Engineering*. **149**(3), 04022259, 2023.
- [16] Kurama Y.C., Weldon Brad D., Shen Q. Experimental evaluation of posttensioned hybrid coupled wall subassemblages. *Journal of Structural Engineering*, **132**(7), 1017-1029, 2006.
- [17] O'Reilly G.J., Goggins J. Experimental testing of a self-centring concentrically braced steel frame. *Engineering Structures*, **238**, 111521, 2021.
- [18] Lettieri A., de La Peña A., Freddi F., Latour M. Damage-free self-centring link for eccentrically braced frames: development and numerical study. *Journal of Constructional Steel Research*, **201**, 107727, 2023.
- [19] Ricles J., Sause R., Garlock M., Zhao C. Post-tensioned Seismic-Resistant Connections for Steel Frames. *Journal of Structural Engineering*, **127**(2), 113–121, 2001.
- [20] Garlock M., Sause R., Ricles J.M. Behavior and design of posttensioned steel frame systems. *Journal of Structural Engineering*, **133**(3), 389–399, 2007.
- [21] Freddi F., Dimopoulos C.A., Karavasilis T.L. Rocking damage-free steel CB with friction devices: design procedure and numerical evaluation. *Earthquake Engineering and Structural Dynamics*, **46**(14), 2281-2300, 2017.
- [22] Elettore E., Freddi F., Latour M., Rizzano G. Design and analysis of a seismic resilient steel MRFs equipped with damage-free self-centering CBs. *Journal of Constructional Steel Research*, **179**, 106543, 2021.
- [23] Kim H.-J., Christopoulos C. (2009). Seismic design procedure and seismic response of post-tensioned self-centering steel frames. *Earthquake Engineering and Structural Dynamics*, **38**, 355–376, 2009.
- [24] Pieroni, L., Freddi, F., Latour M. Effective placement of Self-Centering Damage-Free Connections for Seismic-Resilient Steel Moment Resisting Frames. *Earthquake Engineering & Structural Dynamics*, **51**(5), 1292–1316, 2022.
- [25] Jiang-Yue Xie, Zhenduo Yan, Junrong Liu, Rui Zhang, Ping Xiang, Xianzhong Zhao, Gregory A. MacRae, G. Charles Clifton, Rajesh P. Dhakal, Shahab Ramhormozian, Geoffrey Rodgers, Pierre Quenneville, Liang-Jiu Jia. Low-damage performance of rocking column bases with Belleville Springs for enhanced seismic resilience, *Engineering Structures*, **330**, 119906, 2025.
- [26] Christopoulos C., Filiatrault A., Uang C.-M., Folz B. Posttensioned energy dissipating connections for moment-resisting steel frames. *Journal of Structural Engineering*, **128**(9), 1111–20, 2002.
- [27] Khoo, H.-H., Clifton, C., Butterworth, J. and MacRae, G. Experimental Study of Full-Scale Self-Centering Sliding Hinge Joint Connections with Friction Ring Springs. *Journal of Earthquake Engineering*, **17**(7):972–997, 2013.
- [28] Deng, K., Pan, P. and Wu, S. Experimental study on a self-centering coupling beam eliminating the beam elongation effect. *The Structural Design of Tall and Special Buildings*, **25**(6), 265–277, 2015.

- [29] Garlock, M. M. and Li, J. Steel self-centering moment frames with collector beam floor diaphragms, *Journal of Constructional Steel Research*, **64**(5), 526–538, 2008.
- [30] Elettore E., Lettieri A., Freddi F., Latour M., Rizzano G. Performance-based assessment of seismic-resilient steel MRFs equipped with innovative CB connections. *Structures*, **32**, 1646-1664, 2021.
- [31] Elettore E., Freddi F., Latour M., Rizzano G. Parametric Finite Element Analysis of Self-Centering Column Bases with different Structural Properties. *Journal of Constructional Steel Research*, **199**, 107628, 2022.
- [32] Elettore E., Freddi F., Latour M., Piluso, V., Rizzano G. Pseudo-Dynamic Testing, Repairability, and Resilience Assessment of a Large-Scale Steel Structure Equipped with Self-Centering Column Bases. *Earthquake Engineering and Structural Dynamics*, **53**(9), 2756-2781, 2023.
- [33] ANSI/AISC 341-16 Seismic Provisions for Structural Steel Buildings, American Institute of Steel Construction, Chicago, USA, 2016.